

Supporting Information for

**Rational Designing of Anthocyanidins-Directed Near-Infrared
Two-Photon Fluorescent Probes**

Xiu-e Zhang^a, Xue Wei^b, Wei-Bo Cui^b, Jin-Pu Bai^a, Aynur Matyusup^a, Jing-Fu Guo^{*a}, Hui Li^b
and Ai-Min Ren^{*b}

^aSchool of Physics, Northeast Normal University, Changchun 130024, P.R.China

^bLaboratory of Theoretical and Computational Chemistry, Institute of Theoretical Chemistry,
College of Chemistry, Jilin University, Liutiao Road #2, Changchun 130061, P.R.China

Corresponding Author: Jing-Fu Guo

E-mail: guojf217@nenu.edu.cn

ORCID: 0000-0002-1864-167X

Corresponding Author: Ai-Min Ren

E-mail: renam@jlu.edu.cn

ORCID: 0000-0002-9192-1483

Table of Contents

Theoretical Approaches

1. One-Photon Absorption (OPA)
2. Two-photon Absorption (TPA)
3. Solvation Free Energy

Electronic structures and photophysical properties

4. **Table S1** Calculated one-photon absorption and fluorescent emission spectra properties of **1a** and **1b** by using different functionals and 6-31G(d, p) basis set.
5. **Table S2** Calculated one-photon absorption and fluorescent emission spectra properties of **1a** and **1b** by using different basis sets and B3LYP functional.
6. **Table S3** The one-photon absorption and fluorescent emission spectra properties of all the experimental molecules were calculated by using 6-311+G(d) basis set and B3LYP/TPSSH functionals..
7. **Table S4** Calculated two-photon absorption properties of the **a**-series and **b**-series molecules in aqueous using B3LYP/6-311+G(d) and CAM-B3LYP/6-311+G(d) methods based on the optimized geometries by B3LYP/6-31G(d,p).
8. **Table S5** Calculated molecular OPA and fluorescence emission properties in aqueous and DMSO solvent using B3LYP/6-311+G(d) method.
9. **Table S6** Calculated molecular TPA properties in aqueous and DMSO solvent using B3LYP/6-311+G(d) method.
10. **Table S7** Calculated radiative (k_r) and nonradiative transition rates (k_{ic}) and fluorescence quantum yield (Φ) of the **a**-series and **b**-series molecules in aqueous, DMSO solvent and gas phase.
11. **Table S8** Calculated radiative (k_r) and nonradiative transition rates (k_{ic}) and fluorescence quantum yield (Φ) of the designed molecules in aqueous.
12. **Table S9** Some bond lengths (\AA) and dihedral angles (deg) at the optimized S_0 and S_1 states for all the studied molecules.

13. **Table S10** Calculated reorganization energy (λ) of the studied molecules, in which E_{S_1} and E_{S_0} represent the energies of the excited and ground states, respectively.
14. **Table S11** The one-photon absorption and fluorescence emission properties of the studied molecules (**1a~5a**, **1b** and **1c**) calculated by B3LYP/6-311+G(d) method, including wavelength (λ), Stokes shift, vertical excitation energy (E), transition dipole moment (μ), oscillator intensity (f), transition character.
15. **Table S12** The related transition dipole moments (units in a.u.) of the studied molecules with multiple possible TPA transition channels.
16. **Table S13** Calculated one-photon absorption and fluorescent emission spectra properties of the probe **2a** and the product **LDO-NTR** by using different functionals and 6-31G(d, p) basis set.
17. **Table S14** Calculated one-photon absorption and fluorescent emission spectra properties of the probe **2a** and the product **LDO-NTR** by using different basis sets and B3LYP functional.
18. **Table S15** Calculated one-photon absorption and fluorescence emission properties of the studied probes and product molecules by using B3LYP/6-31G(d, p).
19. **Table S16** The change of natural charge population ($\Delta Q/e$) of each fragment of the studied molecules during the transition, including g stands for the ground state, and e represents the excited state.
20. **Fig. S1** The chemical structures and atomic numbering of the molecules (**1a**, **1b** and **1c**).
21. **Fig. S2** The superimposed structures of the S_0 and S_1 states and the corresponding RMSD values for the studied molecules. (the red and the blue represent the S_0 and S_1 states, respectively.)
22. **Fig. S3** The main frontier molecular orbitals of the studied experimental molecules.
23. **Fig. S4** The main frontier molecular orbitals of the molecules **1a**, **1b** and **1c**.

24. **Fig. S5** The FMO energies of the molecules (**1a**, **1b** and **1c**) by DFT//B3LYP/6-31G(d, p).
25. **Fig. S6** The simulated one-photon absorption and fluorescence emission spectra of the studied molecules (**1a**, **1b** and **1c**).
26. **Fig. S7** The chemical structures of the molecules **2a~5a**.
27. **Fig. S8** The main frontier molecular orbitals of the molecules **2a~5a**.
28. **Fig. S9** The FMO energies of the studied complexes (**2a~5a**) by DFT//B3LYP/6-31G(d, p).
29. **Fig. S10** The simulated one-photon absorption and fluorescence emission spectra of the studied molecules (**2a~5a**).
30. **Fig. S11** The main frontier molecular orbitals of the designed molecules.
31. **Fig. S12** Comparison between the δ^{3SM} calculated by using the three-state model and the δ^{TPA} predicted by the response theory of the studied molecules. Besides, the δ^{ii} is the first item in the three-state model formula. (a)the experimental molecules. (b)the designed molecules.
32. **Fig. S13** Plots of (a) the dipole moment vectors μ and (b) the angle terms X existed in the 3SM of the studied experimental molecules.
33. **Fig. S14** The main frontier molecular orbitals of the studied probes and products.
34. **Fig. S15** Detailed division of the probes and products. (I in green, II in black, III in red)
35. **Fig. S16** The detailed division of electron donor and electron acceptor regions for the probe **LDO-NTR** and **2a-3-NTR**, including the green is the electron acceptor and the red is the electron donor.

Theoretical Methods

1. One-Photon Absorption (OPA)

The OPA transition intensity is calculated by the following formula:¹

$$\delta_{\text{OP}} = \frac{2\omega_f}{3} \sum_{\alpha} |\langle 0 | \mu_{\alpha} | f \rangle|^2 \quad \backslash * \text{ MERGEFORMAT (1)}$$

Here, ω_f is the excitation energy from the ground state S_0 to the singlet excited state S_f , μ_{α} is the electron transition dipole moment and the sum of the x , y and z directions of the molecule.

2. Two-Photon Absorption (TPA)

The TPA cross section (δ_{TP}) determines the TPA intensity and is associated with the TPA transition probability, which can be obtained from the two-photon transition matrix element ($S_{\alpha\beta}$). And the expression of $S_{\alpha\beta}$ is as follows:²

$$S_{\alpha\beta} = \sum_i \left[\frac{\langle 0 | \mu_{\alpha} | i \rangle \langle i | \mu_{\beta} | f \rangle}{\omega_i - \frac{\omega_f}{2}} + \frac{\langle 0 | \mu_{\beta} | i \rangle \langle i | \mu_{\alpha} | f \rangle}{\omega_i - \frac{\omega_f}{2}} \right] \backslash * \text{ MERGEFORMAT}$$

(2)

Where μ_{α} and μ_{β} are dipole moment operators, respectively. ω_i represents the excitation energy from S_0 to S_i , and $\omega_f / 2$ represents half of the excitation energy from S_0 to S_f .

Then, with the help of $S_{\alpha\beta}$, the TPA transition probability can be defined by the following equation:³

$$\delta_{\text{a.u.}} = \frac{1}{30} \sum_{\alpha, \beta} (2S_{\alpha\alpha} S_{\beta\beta}^* + 4S_{\alpha\beta} S_{\beta\alpha}^*) \quad \backslash * \text{ MERGEFORMAT (3)}$$

Finally, the δ_{TP} value can be carried out as follows:⁴

$$\delta_{\text{TP}} = \frac{4\pi^2 a_0^5 \alpha \omega^2}{15c\Gamma} \delta_{\text{au}} \quad \backslash * \text{MERGEFORMAT (4)}$$

Here, α and a_0 represent the fine structure parameter and Bohr radius, respectively. ω and c stand for the photon a_0 energy in atomic units and the speed of light, respectively. Γ refers to the broadening factor of the final state energy level, which is assumed to be 0.1 eV.⁵

3. Solvation Free Energy

The solvation free energy is the difference between the solute free energy in solution and gas phase, which can be calculated by the following formula:^{6,7}

$$\Delta G_{\text{solv}} = G_{\text{solv}} - G_{\text{gas}} \quad \backslash * \text{MERGEFORMAT (5)}$$

Here, G_{solv} and G_{gas} are the energy of the molecule in the solvent and the gas phase, respectively.

Table S1 Calculated one-photon absorption and fluorescent emission spectra properties of **1a** and **1b** in aqueous using different functionals and 6-31G(d, p) basis set.

Functionals	1a				1b			
	$\lambda_{\max,abs}$	f^O	$\lambda_{\max,ems}$	f^e	$\lambda_{\max,abs}$	f^O	$\lambda_{\max,ems}$	f^e
TPSSH	523.02	1.1646	608.35	0.9113	494.88	1.249 6	566.50	0.9895
B3LYP	508.31	1.2163	575.73	1.0207	492.46	1.292 4	555.22	1.1038
PBE0	495.05	1.2585	555.73	1.0889	480.13	1.340 7	538.42	1.1678
M06	494.20	1.2382	551.17	1.0915	481.71	1.307 4	536.71	1.1538
BMK	473.71	1.3473	520.19	1.2304	448.98	1.434 6	492.21	1.3116
M062X	471.02	1.3648	516.53	1.2739	456.02	1.455 9	502.96	1.3505
CAM-B3LYP	464.85	1.3609	514.66	1.2735	449.38	1.458 5	495.50	1.3690
wB97XD	460.64	1.3576	505.55	1.2927	446.86	1.452 6	488.70	1.3805
EXP.	542		601		533		590	

Table S2 Calculated one-photon absorption and fluorescent emission spectra properties of **1a** and **1b** in aqueous using different basis sets and B3LYP functional.

Basis sets	1a				1b			
	$\lambda_{\max,abs}$	f^O	$\lambda_{\max,ems}$	f^e	$\lambda_{\max,abs}$	f^O	$\lambda_{\max,ems}$	f^e
6-31G(d,p)	508.31	1.2163	575.73	1.0207	492.46	1.2924	555.22	1.1038
6-31+G(d)	517.07	1.2455	586.54	1.0429	501.04	1.3235	566.31	1.1268
6-311G(d,p)	513.70	1.2260	582.38	1.0289	497.67	1.3024	562.08	1.1117
6-311+G(d)	519.95	1.2445	590.24	1.0430	503.80	1.3224	569.97	1.1269
6-311++G(d,p)	519.45	1.2461	588.91	1.0447	490.67	1.3456	568.74	1.1289
EXP.	542		601		533		590	

Table S3 The one-photon absorption and fluorescent emission spectra properties of all the experimental molecules in aqueous were calculated by using 6-311+G(d) basis set and B3LYP/TPSSH functionals.

MOL.	Method	Electronic transition	λ/nm	Stokes shift/nm	E/eV	f	Configuration
1a	B3LYP	S ₀ →S ₁	519.95/542 ^{expt}	70.29/59 ^{expt}	2.38	1.2445	H→L 99.02%
		S ₁ →S ₀	590.24/601 ^{expt}		2.10	1.0430	H→L 99.66%

1b	TPSSH	$S_0 \rightarrow S_1$	533.63/542 ^{expt}	88.10/59 ^{expt}	2.32	1.1930	H→L	99.30%
		$S_1 \rightarrow S_0$	621.73/601 ^{expt}		1.99	0.9330	H→L	100%
	B3LYP	$S_0 \rightarrow S_1$	503.80/533 ^{expt}	66.17/57 ^{expt}	2.46	1.3224	H→L	99.10%
		$S_1 \rightarrow S_0$	569.97/590 ^{expt}		2.18	1.1269	H→L	99.66%
2a	TPSSH	$S_0 \rightarrow S_1$	504.21/533 ^{expt}	74.69/57 ^{expt}	2.46	1.2815	H→L	99.30%
		$S_1 \rightarrow S_0$	578.90/590 ^{expt}		2.14	1.0094	H→L	99.83%
	B3LYP	$S_0 \rightarrow S_1$	551.59/574 ^{expt}	92.59/59 ^{expt}	2.25	1.4032	H→L	99.10%
		$S_1 \rightarrow S_0$	644.18/633 ^{expt}		1.92	1.1251	H→L	99.76%
2b	TPSSH	$S_0 \rightarrow S_1$	572.09/574 ^{expt}	116.96/59 ^{expt}	2.17	1.3304	H→L	99.53%
		$S_1 \rightarrow S_0$	689.05/633 ^{expt}		1.80	0.9932	H→L	100%
	B3LYP	$S_0 \rightarrow S_1$	535.52/566 ^{expt}	84.42/54 ^{expt}	2.32	1.4698	H→L	99.24%
		$S_1 \rightarrow S_0$	619.94/620 ^{expt}		2.00	1.2074	H→L	99.77%
3a	TPSSH	$S_0 \rightarrow S_1$	555.60/566 ^{expt}	82.17/54 ^{expt}	2.23	1.3862	H→L	99.50%
		$S_1 \rightarrow S_0$	637.77/620 ^{expt}		1.94	1.0678	H→L	100%
	B3LYP	$S_0 \rightarrow S_1$	545.60/584 ^{expt}	69.01/55 ^{expt}	2.27	1.3689	H→L	98.61%
		$S_1 \rightarrow S_0$	614.61/639 ^{expt}		2.02	1.0839	H→L	99.03%
3b	TPSSH	$S_0 \rightarrow S_1$	558.95/584 ^{expt}	102.14/55 ^{expt}	2.22	1.3240	H→L	97.91%
		$S_1 \rightarrow S_0$	661.09/639 ^{expt}		1.88	0.9351	H→L	99.41%
	B3LYP	$S_0 \rightarrow S_1$	526.87/572 ^{expt}	66.13/48 ^{expt}	2.35	1.4499	H→L	98.57%
		$S_1 \rightarrow S_0$	593.00/620 ^{expt}		2.09	1.2102	H→L	98.99%
TPSSH	$S_0 \rightarrow S_1$	547.74/572 ^{expt}	82.10/48 ^{expt}	2.26	1.3421	H→L	97.10%	
	$S_1 \rightarrow S_0$	629.84/620 ^{expt}		1.97	1.0878	H→L	99.20%	

Table S4 Calculated two-photon absorption properties of the **a**-series and **b**-series molecules in aqueous using B3LYP/6-311+G(d) and CAM-B3LYP/6-311+G(d) methods based on the optimized geometries by B3LYP/6-31G(d,p).

MOL.	Method	λ_{TPA}/nm	δ_{TPA}/GM	Transition character		
1a	B3LYP/6-311+G(d)	953.73	14.56	$S_0 \rightarrow S_1$	H→L	99.02%
		744.65	110.48	$S_0 \rightarrow S_2$	H-1→L	92.48%
	CAM-B3LYP/6-311+G(d)	891.98	20.20	$S_0 \rightarrow S_1$	H→L	95.54%
		635.82	334.00	$S_0 \rightarrow S_2$	H-1→L	86.73%
1b	B3LYP/6-311+G(d)	901.71	11.30	$S_0 \rightarrow S_1$	H→L	99.10%
		694.59	164.33	$S_0 \rightarrow S_3$	H-2→L	93.36%

		843.44	16.90	$S_0 \rightarrow S_1$	H→L	95.93%
	CAM-B3LYP/6-311+G(d)	601.87	366.00	$S_0 \rightarrow S_2$	H-1→L	85.16%
		1008.01	27.66	$S_0 \rightarrow S_1$	H→L	99.10%
	B3LYP/6-311+G(d)	746.90	185.73/161.8 ^{expt[24]}	$S_0 \rightarrow S_2$	H-1→L	81.63%
2a		928.73	34.90	$S_0 \rightarrow S_1$	H→L	94.61%
	CAM-B3LYP/6-311+G(d)	635.82	581.00/161.8 ^{expt[24]}	$S_0 \rightarrow S_2$	H-1→L	75.56%
		980.12	22.60	$S_0 \rightarrow S_1$	H→L	99.24%
	B3LYP/6-311+G(d)	714.61	323.74	$S_0 \rightarrow S_2$	H-1→L	83.07%
		898.44	29.60	$S_0 \rightarrow S_1$	H→L	95.27%
2b		600.41	578.00	$S_0 \rightarrow S_3$	H-2→L	42.65%
	CAM-B3LYP/6-311+G(d)				H-1→L	17.77%
					H-4→L	16.55%
		999.88	36.45	$S_0 \rightarrow S_1$	H→L	98.61%
	B3LYP/6-311+G(d)	731.47	181.85	$S_0 \rightarrow S_3$	H-2→L	77.50%
3a					H-3→L	15.43%
		918.41	57.10	$S_0 \rightarrow S_1$	H→L	93.92%
	CAM-B3LYP/6-311+G(d)	624.61	595.00	$S_0 \rightarrow S_3$	H-2→L	75.51%
		968.63	24.82	$S_0 \rightarrow S_1$	H→L	98.57%
	B3LYP/6-311+G(d)	704.46	236.01	$S_0 \rightarrow S_3$	H-2→L	70.84%
					H-3→L	17.28%
3b		885.61	41.10	$S_0 \rightarrow S_1$	H→L	94.86%
		587.61	554.00	$S_0 \rightarrow S_4$	H-3→L	33.35%
	CAM-B3LYP/6-311+G(d)				H-5→L	25.43%
					H-2→L	22.71%

Table S5 Calculated molecular OPA and fluorescence emission properties in aqueous and DMSO solvent using B3LYP/6-311+G(d) method.

MOL.	Solvent	Electronic transition	λ /nm	Stokes shift/nm	E /eV	f	Transition character	
1a	aqueous	S ₀ →S ₁	519.95/542 ^{expt}	70.29/59 ^{expt}	2.38	1.2445	H→L	99.02%
		S ₁ →S ₀	590.24/601 ^{expt}		2.10	1.0430	H→L	99.66%
	DMSO	S ₀ →S ₁	518.98/542 ^{expt}	70.08/59 ^{expt}	2.39	1.2378	H→L	99.02%
		S ₁ →S ₀	589.06/601 ^{expt}		2.10	1.0357	H→L	99.67%
1b	aqueous	S ₀ →S ₁	503.80/533 ^{expt}	66.17/57 ^{expt}	2.46	1.3224	H→L	99.10%
		S ₁ →S ₀	569.97/590 ^{expt}		2.18	1.1269	H→L	99.66%
	DMSO	S ₀ →S ₁	502.85/533 ^{expt}	65.95/57 ^{expt}	2.47	1.3151	H→L	99.10%
		S ₁ →S ₀	568.80/590 ^{expt}		2.18	1.1197	H→L	99.67%
2a	aqueous	S ₀ →S ₁	551.59/574 ^{expt}	92.59/59 ^{expt}	2.25	1.4032	H→L	99.10%
		S ₁ →S ₀	644.18/633 ^{expt}		1.92	1.1251	H→L	99.76%
	DMSO	S ₀ →S ₁	550.54/574 ^{expt}	92.44/59 ^{expt}	2.25	1.3968	H→L	99.11%
		S ₁ →S ₀	642.98/633 ^{expt}		1.93	1.1182	H→L	99.78%
2b	aqueous	S ₀ →S ₁	535.52/566 ^{expt}	84.42/54 ^{expt}	2.32	1.4698	H→L	99.24%
		S ₁ →S ₀	619.94/620 ^{expt}		2.00	1.2074	H→L	99.77%
	DMSO	S ₀ →S ₁	534.49/566 ^{expt}	84.38/54 ^{expt}	2.32	1.4638	H→L	99.25%
		S ₁ →S ₀	618.87/620 ^{expt}		2.00	1.2006	H→L	99.79%
3a	aqueous	S ₀ →S ₁	545.60/584 ^{expt}	69.01/55 ^{expt}	2.27	1.3689	H→L	98.61%
		S ₁ →S ₀	614.61/639 ^{expt}		2.02	1.0839	H→L	99.03%
	DMSO	S ₀ →S ₁	544.59/584 ^{expt}	69.28/55 ^{expt}	2.28	1.3625	H→L	98.60%
		S ₁ →S ₀	613.87/639 ^{expt}		2.02	1.0759	H→L	99.04%
3b	aqueous	S ₀ →S ₁	526.87/572 ^{expt}	66.13/48 ^{expt}	2.35	1.4499	H→L	98.57%
		S ₁ →S ₀	593.00/620 ^{expt}		2.09	1.2102	H→L	98.99%
	DMSO	S ₀ →S ₁	525.97/572 ^{expt}	66.09/48 ^{expt}	2.36	1.4427	H→L	98.55%
		S ₁ →S ₀	592.06/620 ^{expt}		2.09	1.2029	H→L	98.99%

Note: experimental values are from reference^[24].

Table S6 Calculated molecular TPA properties in aqueous and DMSO solvent using B3LYP/6-311+G(d) method.

MOL.	Solvent	$\lambda_{\text{TPA}}/\text{nm}$	$\delta_{\text{TPA}}/\text{GM}$	Transition character		
1a	aqueous	953.73	14.56	$S_0 \rightarrow S_1$	H \rightarrow L	99.02%
		744.65	110.48	$S_0 \rightarrow S_2$	H-1 \rightarrow L	92.48%
	DMSO	964.86	17.30	$S_0 \rightarrow S_1$	H \rightarrow L	99.02%
		744.65	151.00	$S_0 \rightarrow S_2$	H-1 \rightarrow L	92.40%
1b	aqueous	901.71	11.30	$S_0 \rightarrow S_1$	H \rightarrow L	99.10%
		694.59	164.33	$S_0 \rightarrow S_3$	H-2 \rightarrow L	93.36%
	DMSO	935.74	11.70	$S_0 \rightarrow S_1$	H \rightarrow L	99.10%
		720.84	179.00	$S_0 \rightarrow S_2$	H-1 \rightarrow L	93.04%
2a	aqueous	1008.01	27.66	$S_0 \rightarrow S_1$	H \rightarrow L	99.10%
		746.90	185.73	$S_0 \rightarrow S_2$	H-1 \rightarrow L	81.63%
	DMSO	1020.45	33.00	$S_0 \rightarrow S_1$	H \rightarrow L	1020.45
		749.15	247.00	$S_0 \rightarrow S_2$	H-1 \rightarrow L	749.15
2b	aqueous	980.12	22.60	$S_0 \rightarrow S_1$	H \rightarrow L	99.24%
		714.61	323.74	$S_0 \rightarrow S_2$	H-1 \rightarrow L	83.07%
	DMSO	991.88	26.60	$S_0 \rightarrow S_1$	H \rightarrow L	991.88
		716.68	433.00	$S_0 \rightarrow S_2$	H-1 \rightarrow L	716.68
3a	aqueous	999.88	36.45	$S_0 \rightarrow S_1$	H \rightarrow L	98.61%
		731.47	181.85	$S_0 \rightarrow S_3$	H-2 \rightarrow L	77.50%
	DMSO	1016.27	44.50	$S_0 \rightarrow S_1$	H \rightarrow L	98.60%
		733.64	235.00	$S_0 \rightarrow S_3$	H-2 \rightarrow L	76.45%
3b	aqueous	968.63	24.82	$S_0 \rightarrow S_1$	H \rightarrow L	98.57%
		704.46	236.01	$S_0 \rightarrow S_3$	H-2 \rightarrow L	70.84%
	DMSO	980.12	30.80	$S_0 \rightarrow S_1$	H \rightarrow L	98.55%
		706.47	313.00	$S_0 \rightarrow S_3$	H-2 \rightarrow L	69.49%
				H-3 \rightarrow L	18.81%	

In order to confirm the designed molecules have great potential to be excellent probe, the radiative and nonradiative transition rates were also assessed using MOMAP software currently available and obtained their fluorescence quantum yields in the frame of the harmonic oscillator approximation. The calculated results are collected in **Table S7-S8**. Unfortunately, the calculated fluorescence quantum yield of ca. 0.0528% of **2a** obtained is far from the experimental values (55%^{expt[24]}). It is perhaps due to the specificity of the molecular structures (during the excitation process, the molecular structures are distorted to certain extent and the harmonic oscillator approximation is no longer applicable for this situation), which makes the calculated nonradiative transition rate biased seriously and ultimately leads to the artificial extremely low fluorescence quantum yield. However, the results from **Table S8** still confirmed that the fluorescence quantum yields of our designed **2a-1** and **2a-3** molecules are substantially improved compared with the experimental molecule **2a**. This implies that our design strategy is effective.

Table S7 Calculated radiative (k_r) and nonradiative transition rates (k_{ic}) and fluorescence quantum yield (Φ) of the **a**-series and **b**-series molecules in aqueous, DMSO solvent and gas phase.

MOL.	Solvent	k_r/S^{-1}	k_{ic}/S^{-1}	Φ
1a	aqueous	1.53×10^8	2.61×10^{11}	0.0586%
	DMSO	1.56×10^8	1.47×10^{11}	0.1059%
	gas	1.00×10^8	2.36×10^{10}	0.4226%
1b	aqueous	2.15×10^8	7.05×10^{10}	0.3044%
	DMSO	2.00×10^8	7.05×10^{10}	0.2831%
	gas	1.26×10^8	1.16×10^{10}	1.0684%
2a	aqueous	1.11×10^8	2.11×10^{11}	0.0528%(55% ^{expt[24]})
	DMSO	1.10×10^8	2.25×10^{11}	0.0488%(55% ^{expt[24]})
	gas	6.16×10^7	1.05×10^{11}	0.0586%

2b	aqueous	1.67×10^8	2.13×10^{10}	0.7791%
	DMSO	1.59×10^8	2.05×10^{10}	0.7685%
	gas	8.92×10^7	3.14×10^{10}	0.2831%
3a	aqueous	1.43×10^8	6.78×10^9	2.0614%
	DMSO	1.41×10^8	8.04×10^9	1.7210%
	gas	5.15×10^8	1.72×10^{11}	0.2983%
3b	aqueous	1.75×10^8	4.35×10^9	3.8598%
	DMSO	1.74×10^8	4.66×10^9	3.5930%
	gas	6.26×10^8	8.37×10^{10}	0.7421%

Table S8 Calculated radiative (k_r) and nonradiative transition rates (k_{ic}) and fluorescence quantum yield (Φ) of the designed molecules in aqueous.

MOL.	k_r/S^{-1}	k_{ic}/S^{-1}	Φ
2a	1.11×10^8	2.11×10^{11}	0.0528%(55% ^{exp(24)})
2a-1	1.20×10^8	4.38×10^{10}	0.2721%
2a-2	3.70×10^7	1.27×10^{12}	0.0029%
2a-3	1.53×10^8	1.84×10^{10}	0.8245%
2a-4	1.17×10^6	3.74×10^{11}	0.0003%
2a-5	1.05×10^8	5.48×10^{11}	0.0192%

Table S9 Some bond lengths (Å) and dihedral angles (deg) at the optimized S₀ and S₁ states for all the studied molecules.

MOL.	O ₁ -C ₂	C ₂ -C ₃	C ₃ -C ₁₀	C ₁₀ -C _n ^a	C ₂ -C _n ^b	DHA1 ^c	DHA2 ^d	DHA3 ^e	DHA4 ^f	DHA5 ^g
1a-S ₀	1.3422	1.4194	1.4291	2.9125	1.4221	-148.02	71.27	-12.92	1.81	-10.77
1a-S ₁	1.3643	1.4612	1.4240	2.9238	1.3778	-151.26	66.94	-14.70	5.80	-12.80
1b-S ₀	1.3297	1.4123	1.4255	2.3640	1.4130	177.62	78.32	0.38	3.55	0.81
1b-S ₁	1.3514	1.4456	1.4196	2.3724	1.3774	175.07	57.41	0.32	8.88	2.39
1c-S ₀	1.3465	1.4267	1.4221	3.0120	1.4092	-	61.55	0.67	4.43	1.36
1c-S ₁	1.3650	1.4714	1.4146	3.0379	1.3627	-	50.34	2.71	10.16	3.74
2a-S ₀	1.3442	1.4152	1.4295	2.9134	1.4259	-147.73	71.76	-12.49	2.33	-10.28
2a-S ₁	1.3616	1.4654	1.4164	2.9216	1.3766	-151.22	69.09	-15.16	5.51	-13.68
2b-S ₀	1.3300	1.4049	1.4260	2.3675	1.4220	178.08	66.24	-0.23	2.26	0.60
2b-S ₁	1.3470	1.4503	1.4125	2.3722	1.3761	175.11	56.60	0.31	7.54	2.25
3a-S ₀	1.3451	1.4214	1.4263	2.9138	1.4172	-149.18	112.11	-12.80	-1.20	-11.73
3a-S ₁	1.3668	1.4661	1.4175	2.9239	1.3736	-146.18	121.44	-17.20	-3.12	-17.10
3b-S ₀	1.3305	1.4093	1.4243	2.3677	1.4168	177.35	66.06	0.06	0.51	1.01
3b-S ₁	1.3512	1.4494	1.4139	2.3746	1.3760	174.75	55.47	0.48	1.31	2.64
2a-1-S ₀	1.3488	1.4104	1.4332	2.9305	1.4274	-147.04	72.62	-13.37	2.22	-10.14
2a-1-S ₁	1.3600	1.4664	1.4149	2.9367	1.3749	-149.53	67.09	-15.99	6.20	-14.17
2a-2-S ₀	1.3396	1.4243	1.4234	2.9132	1.4189	146.83	70.43	12.95	2.54	11.29
2a-2-S ₁	1.3638	1.4622	1.4190	2.9243	1.3778	147.40	62.82	15.67	6.46	15.22
2a-3-S ₀	1.3438	1.4089	1.4342	2.9311	1.4326	-147.41	74.23	-13.06	1.74	-9.78
2a-3-S ₁	1.3543	1.4621	1.4167	2.9355	1.3809	-149.53	70.66	-16.05	4.53	-14.08
2a-4-S ₀	1.3345	1.4211	1.4257	2.9125	1.4267	-146.95	69.86	-12.62	2.05	-10.55
2a-4-S ₁	1.3780	1.4291	1.4237	2.9222	1.4069	-152.06	80.82	-13.71	2.82	-10.93
2a-5-S ₀	1.3390	1.4136	1.4305	2.9138	1.4318	-148.49	73.00	-12.36	1.81	-10.15
2a-5-S ₁	1.3574	1.4563	1.4192	2.9186	1.3859	-151.34	73.87	-14.93	3.62	-13.14

^a: C_n refers to C₁₃ in **a**-series molecules, C₁₂ in **b**-series molecules, respectively.

^b: C_n refers to C₁₃ in **a**-series molecules, C₁₂ in **b**-series molecules and C₁₁ in **c**-series molecules, respectively.

^c: DHA1 is the dihedral angle between the atoms 6-13-12-11 (**a**-series molecules) or 6-12-11-10 (**b**-series molecules).

^d: DHA2 is the dihedral angle between the atoms 5-6-7-8.

^e: DHA3 is the dihedral angle between the atoms 13-2-3-10 (**a**-series molecules) or 12-2-3-10 (**b**-series molecules) or 11-2-3-10 (**c**-series molecules).

^f: DHA4 is the dihedral angle between the atoms 6-7-8-9.

^g: DHA5 is the dihedral angle between the atoms 1-2-3-4.

Table S10 Calculated reorganization energy (λ) of the studied molecules, in which E_{S_1} and E_{S_0} represent the energies of the excited and ground states, respectively.

MOL.	$E_{S_1}/\text{Hartree}$	$E_{S_0}/\text{Hartree}$	λ/cm^{-1}
1a	-1280.9625	-1280.9683	1262.04
1b	-1241.6442	-1241.6496	1187.46
1c	-1203.5270	-1203.5326	1240.38
2a	-1819.1649	-1819.1711	1370.09
2b	-1779.8440	-1779.8501	1338.33
3a	-1745.1281	-1745.1332	1101.87
3b	-1705.8060	-1705.8109	1089.32

Table S11 The one-photon absorption and fluorescence emission properties of the studied molecules (**2a~5a**) calculated by B3LYP/6-311+G(d) method, including wavelength (λ), Stokes shift, vertical excitation energy (E), transition dipole moment (μ), oscillator intensity (f), transition character.

MOL.	Electronic transition	λ/nm	Stokes shift/nm	E/eV	$\mu/\text{a.u.}$	f	Transition character	
1a	$S_0 \rightarrow S_1$	519.95/542 ^{expt}	70.29/59 ^{expt}	2.38	4.62	1.2445	H→L	99.02%
	$S_1 \rightarrow S_0$	590.24/601 ^{expt}		2.10	4.50	1.0430	H→L	99.66%
1b	$S_0 \rightarrow S_1$	503.80/533 ^{expt}	66.17/57 ^{expt}	2.46	4.68	1.3224	H→L	99.10%
	$S_1 \rightarrow S_0$	569.97/590 ^{expt}		2.18	4.60	1.1269	H→L	99.66%
1c	$S_0 \rightarrow S_1$	520.19	71.78	2.38	4.62	1.2448	H→L	99.07%
	$S_1 \rightarrow S_0$	591.97		2.09	4.38	0.9831	H→L	99.61%
2a	$S_0 \rightarrow S_1$	551.59/574 ^{expt}	92.59/59 ^{expt}	2.25	5.05	1.4032	H→L	99.10%
	$S_1 \rightarrow S_0$	644.18/633 ^{expt}		1.92	4.88	1.1251	H→L	99.76%
3a	$S_0 \rightarrow S_1$	545.60/584 ^{expt}	69.01/55 ^{expt}	2.27	4.96	1.3689	H→L	98.61%
	$S_1 \rightarrow S_0$	614.61/639 ^{expt}		2.02	4.68	1.0839	H→L	99.03%
4a	$S_0 \rightarrow S_1$	523.63	67.02	2.37	4.76	1.3121	H→L	99.17%
	$S_1 \rightarrow S_0$	590.65		2.10	4.66	1.1144	H→L	99.71%
5a	$S_0 \rightarrow S_1$	547.54	80.75	2.26	4.90	1.3347	H→L	98.98%
	$S_1 \rightarrow S_0$	628.29		1.97	4.72	1.0792	H→L	99.64%

Table S12 The related transition dipole moments (units in a.u.) of the studied molecules with multiple possible TPA transition channels.

MOL.	μ^{01}	μ^{13}	μ^{02}	μ^{23}		
1b	3.92	1.59	0.44	0.63		
3a	4.20	1.18	0.93	0.38		
3b	4.25	1.34	1.06	0.90		
2a-4	2.78	0.70	4.06	2.62		
2a-5	3.74	1.29	2.99	2.33		
MOL.	μ^{01}	μ^{14}	μ^{02}	μ^{24}	μ^{03}	μ^{34}
2a-1	4.41	1.09	0.48	1.11	0.80	0.78
2a-3	4.89	2.06	0.57	1.00	0.48	1.25

Table S13 Calculated one-photon absorption and fluorescent emission spectra properties of the probe **2a** and the product **LDO-NTR** by using different functionals and 6-31G(d, p) basis set.

Functionals	2a				LDO-NTR			
	$\lambda_{\max, \text{abs}}$	f^O	$\lambda_{\max, \text{ems}}$	f^e	$\lambda_{\max, \text{abs}}$	f^O	$\lambda_{\max, \text{ems}}$	f^e
TPSSH	513.00	1.0298	674.45	0.9817	720.20	0.0000	1414.91	0.0000
B3LYP	540.17	1.3932	629.14	1.1129	558.41	0.0000	938.54	0.0000
PBE0	526.96	1.4422	605.16	1.1949	471.00	0.0001	731.68	0.0000
M06	524.85	1.4271	594.13	1.2125	462.24	0.0001	698.14	0.0000
BMK	499.46	1.5549	555.55	1.3811	362.65	0.0004	508.06	0.0000
M062X	494.89	1.5763	544.92	1.4467	309.39	0.0000	558.32	0.0000
CAM-B3LYP	486.53	1.5768	541.48	1.4551	307.04	0.0000	549.43	0.0000
wB97XD	482.25	1.5774	531.61	1.4837	306.61	0.0000	547.15	0.0000
EXP.	574		633		561		624	

Table S14 Calculated one-photon absorption and fluorescent emission spectra properties of the probe **2a** and the product **LDO-NTR** by using different basis sets and B3LYP functional.

Basis sets	2a				LDO-NTR			
	$\lambda_{\max, \text{abs}}$	f^O	$\lambda_{\max, \text{ems}}$	f^e	$\lambda_{\max, \text{abs}}$	f^O	$\lambda_{\max, \text{ems}}$	f^e
6-31G(d,p)	540.17	1.3932	629.14	1.1129	558.41	0.0000	938.54	0.0000
6-31+G(d)	549.09	1.4031	641.10	1.1233	626.85	0.0000	1125.54	0.0000
6-311G(d,p)	546.28	1.4053	637.04	1.1247	565.64	0.0000	952.46	0.0000
6-311+G(d)	551.59	1.4032	644.18	1.1251	628.03	0.0000	1126.72	0.0000
6-311++G(d,p)	551.69	1.4034	644.17	1.1251	628.87	0.0000	1128.24	0.0000
EXP.	574		633		561		624	

Table S15 Calculated one-photon absorption and fluorescence emission properties of the studied probes and product molecules by using B3LYP/6-31G(d, p).

Molecules	Electronic transition	λ/nm	E/eV	f	Configuration	
Absorption						
LDO-NTR	$S_0 \rightarrow S_1$	558.41/561 ^{expt}	2.22	0.0000	H→L	99.96%
	$S_0 \rightarrow S_2$	392.56	3.16	0.0078	H→L+1	98.22%
	$S_0 \rightarrow S_3$	383.42	3.23	0.0042	H-1→L	97.37%
	$S_0 \rightarrow S_4$	346.49	3.58	0.7225	H→L+2	98.36%
2a	$S_0 \rightarrow S_1$	540.17/574 ^{expt}	2.30	1.3932	H→L	99.21%
2a-3-NTR	$S_0 \rightarrow S_1$	624.64	1.98	0.0000	H→L	99.98%
	$S_0 \rightarrow S_2$	443.48	2.80	0.2085	H→L+1	98.48%
2a-3	$S_0 \rightarrow S_1$	571.12	2.17	1.7092	H→L	97.09%
Emission						
LDO-NTR	$S_1 \rightarrow S_0$	938.54/624 ^{expt}	1.32	0.0000	H→L	99.97%
2a	$S_1 \rightarrow S_0$	629.14/633 ^{expt}	1.97	1.1129	H→L	99.92%
2a-3-NTR	$S_1 \rightarrow S_0$	1129.69	1.10	0.0000	H→L	99.98%
2a-3	$S_1 \rightarrow S_0$	676.49	1.83	1.4677	H→L	99.35%

Table S16. The change of natural charge population ($\Delta Q/e$) of each fragment of the studied molecules during the transition, including g stands for the ground state, and e represents the excited state.

MOL.		I	II	III
LDO-NTR	Q_g	-0.1906	0.1731	0.0175
	Q_e	-1.1458	0.8246	0.3212
	ΔQ	-0.9552	0.6515	0.3038
2a	Q_g	-0.1376	0.9907	0.1469
	Q_e	-0.1308	0.8779	0.2528
	ΔQ	0.0068	-0.1128	0.1060
2a-3-NTR	Q_g	-0.1968	0.1152	0.0817
	Q_e	-1.1555	0.6931	0.4624
	ΔQ	-0.9587	0.5779	0.3807
2a-3	Q_g	-0.1576	0.3515	0.8061
	Q_e	-0.1443	0.2684	0.8759
	ΔQ	0.0133	-0.0831	0.0698

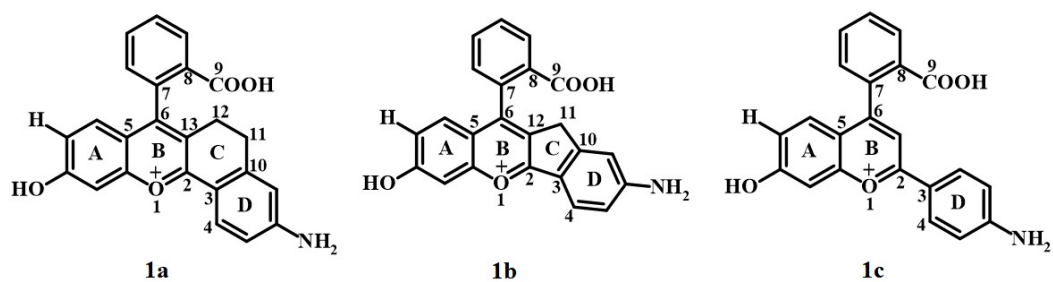


Fig. S1 The chemical structures and atomic numbering of the molecules (**1a**, **1b** and **1c**).

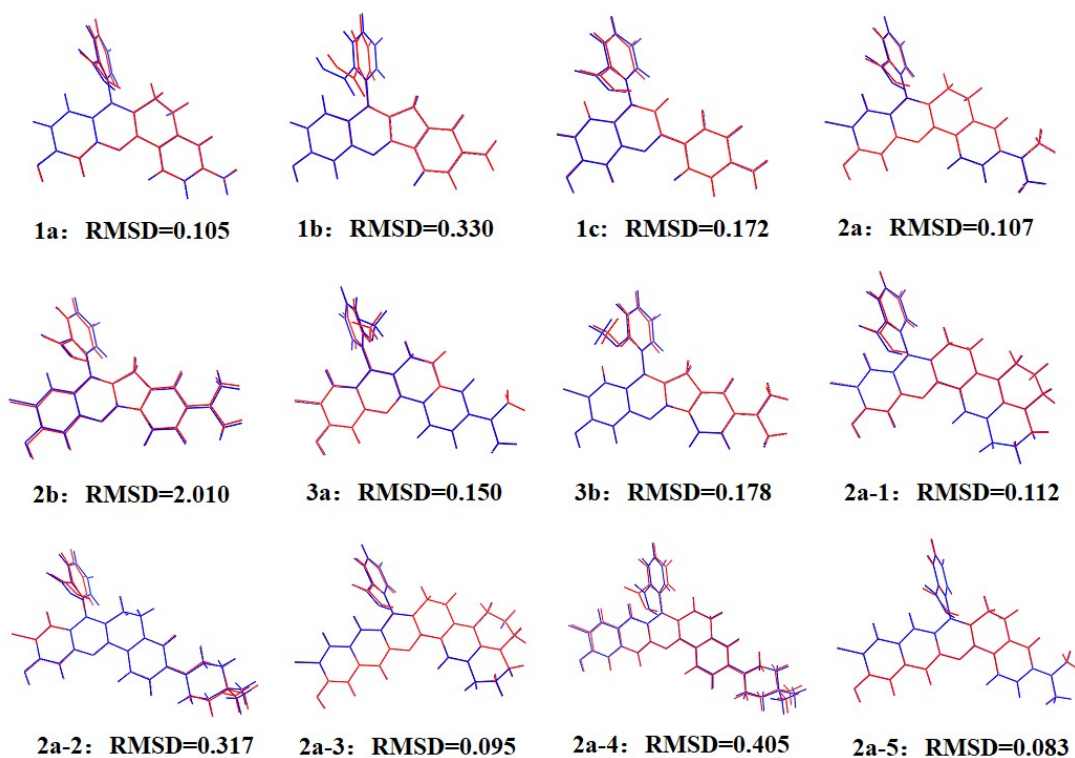


Fig. S2 The superimposed structures of the S_0 and S_1 states and the corresponding RMSD values for the studied molecules. (the red and the blue represent the S_0 and S_1 states, respectively.)

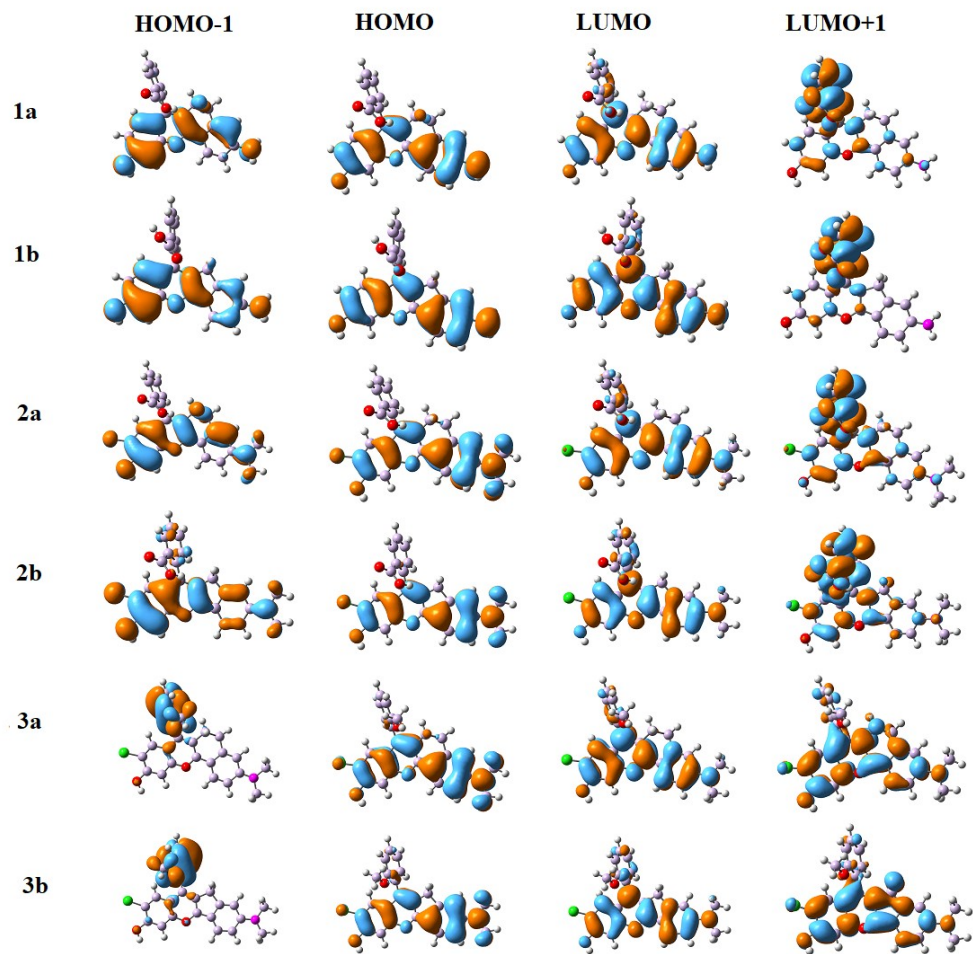


Fig. S3 The main frontier molecular orbitals of the studied experimental molecules.

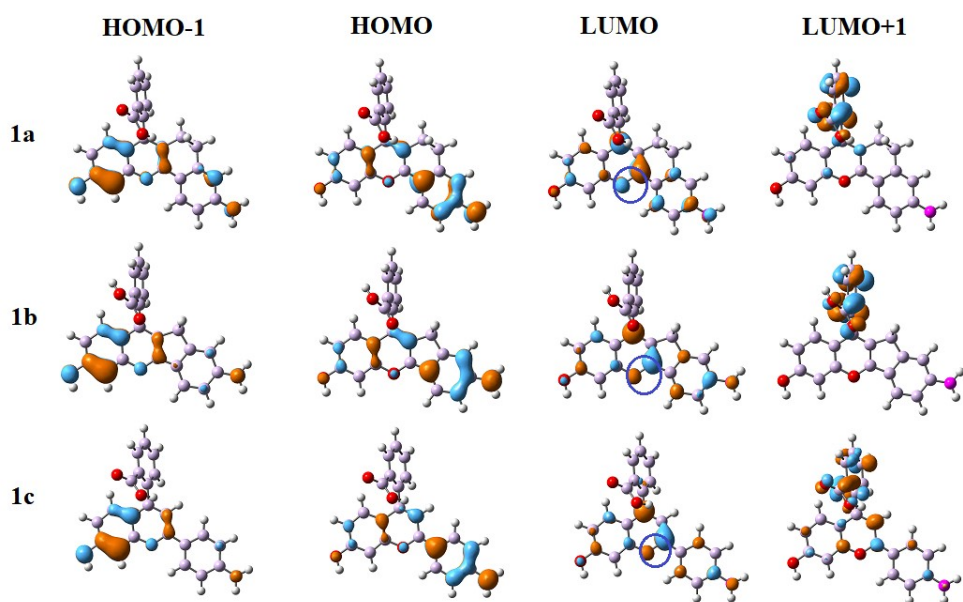


Fig. S4 The main frontier molecular orbitals of the molecules 1a, 1b and 1c.

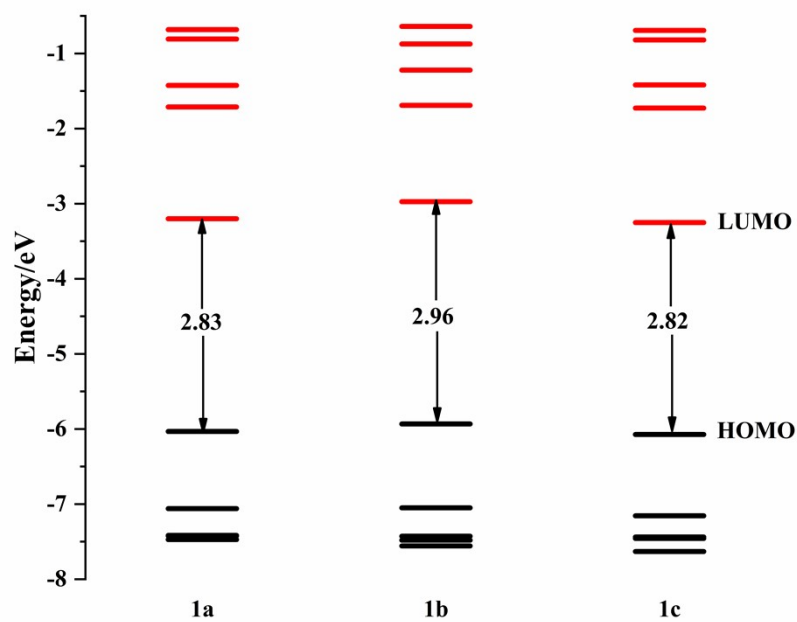


Fig. S5 The FMO energies of the molecules (**1a**, **1b** and **1c**) by DFT//B3LYP/6-31G(d, p).

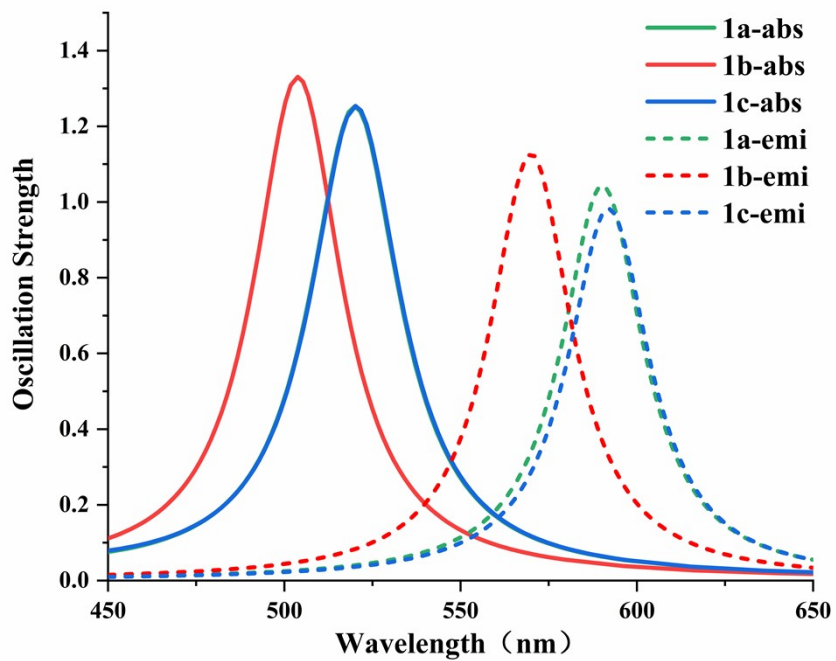


Fig. S6 The simulated one-photon absorption and fluorescence emission spectra of the studied molecules (**1a**, **1b** and **1c**).

In order to find suitable molecular design strategies for the purpose of improving the photophysical properties of **2a** molecules (such as emission wavelength, Stokes shift and TPA cross sections), the **2a~5a** molecules with different substituents are investigated and their chemical structures are shown in **Fig. S7**. The calculated frontier molecular orbitals and the corresponding energy levels are shown in **Fig. S8** and **Fig. S9**. The results indicate that for **2a** and **4a** molecules with different R₁ substituents, the former has a significantly smaller HOMO-LUMO gap owing to the fact that -N(CH₃)₂ has a stronger electron-donating capacity than -NH₂ group, which in turn leads to a higher HOMO energy levels. It's observed that **2a** and **3a** with different R₃ substituents have the similar situation as the above discussion. And for **2a** and **5a** molecules with different R₂ substituents, since -Cl has a greater electron-withdrawing capacity than -H, which make **2a** has a lower LUMO energy level, ultimately resulting in a smaller $\Delta E_{\text{HOMO-LUMO}}$. Especially, we find that the R₁ substitution site is able to regulate the HOMO-LUMO gap to a greater extent, which further facilitates the achievement of long-wavelength emission. But is it really what we assume?

To verify the above speculation, the OPA and fluorescence emission properties of the molecules **2a~5a** are calculated, and the specific values and simulated spectra are summarized in **Table S11** and **Fig. S10**, respectively. Unsurprisingly, the **4a** and **2a** molecules differ only in the R₁ substituent, and the OPA and emission spectra as well as the Stokes shift changes are more significant. This phenomenon cause us to think deeply, if the introduction of appropriate substituents in the R₁ site can better achieve

our desired results? Therefore, a novel molecular design strategy is proposed, leading to the **2a-n** ($n=1-5$) series.

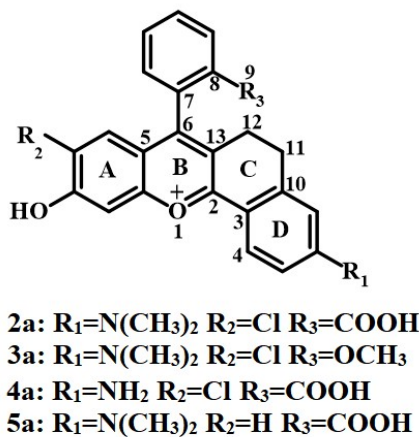


Fig. S7 The chemical structures of the molecules **2a~5a**.

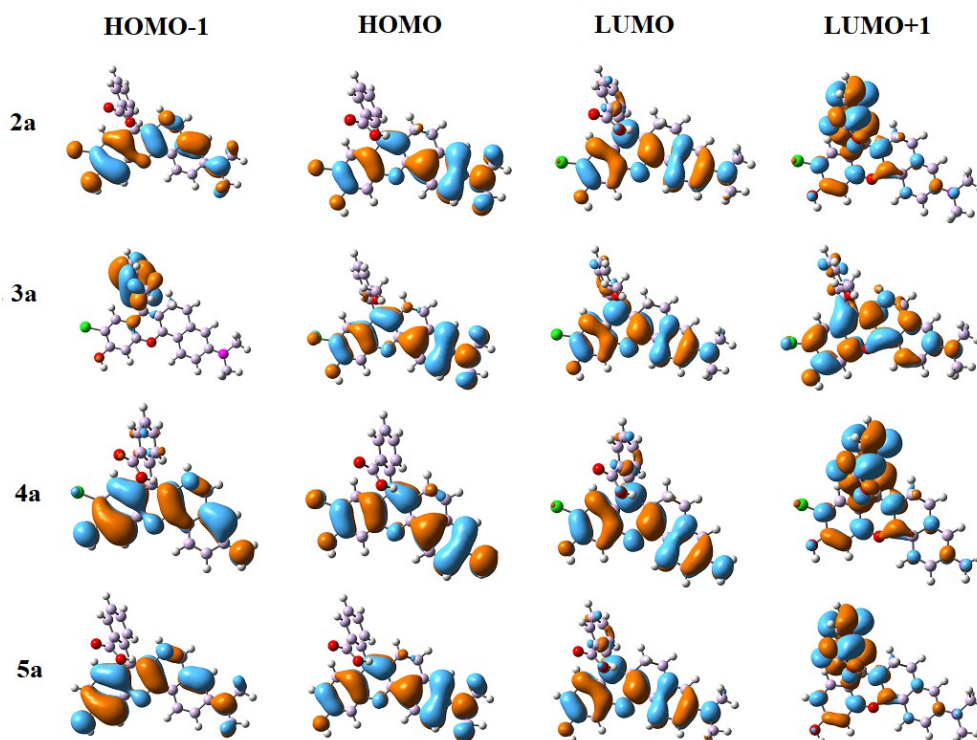


Fig. S8 The main frontier molecular orbitals of the molecules **2a~5a**.

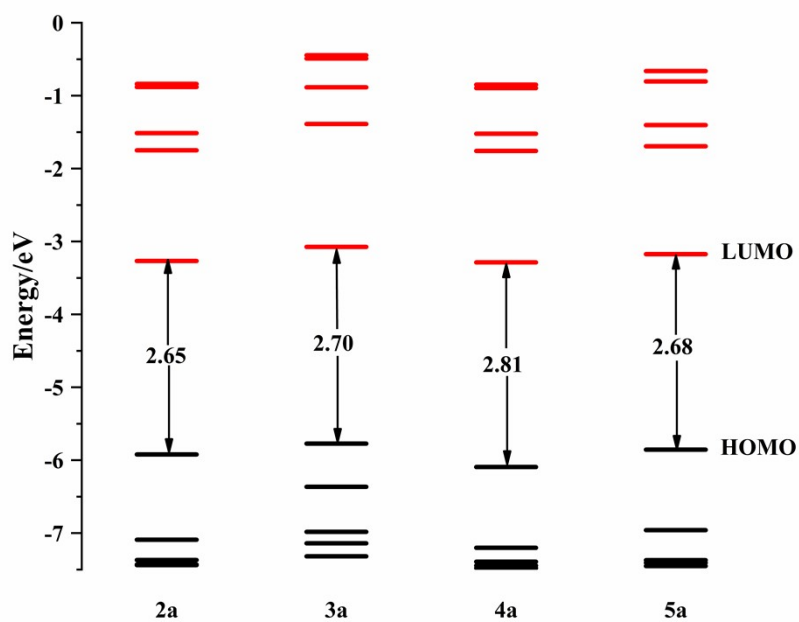


Fig. S9 The FMO energies of the studied complexes (**2a~5a**) by DFT//B3LYP/6-31G(d, p).

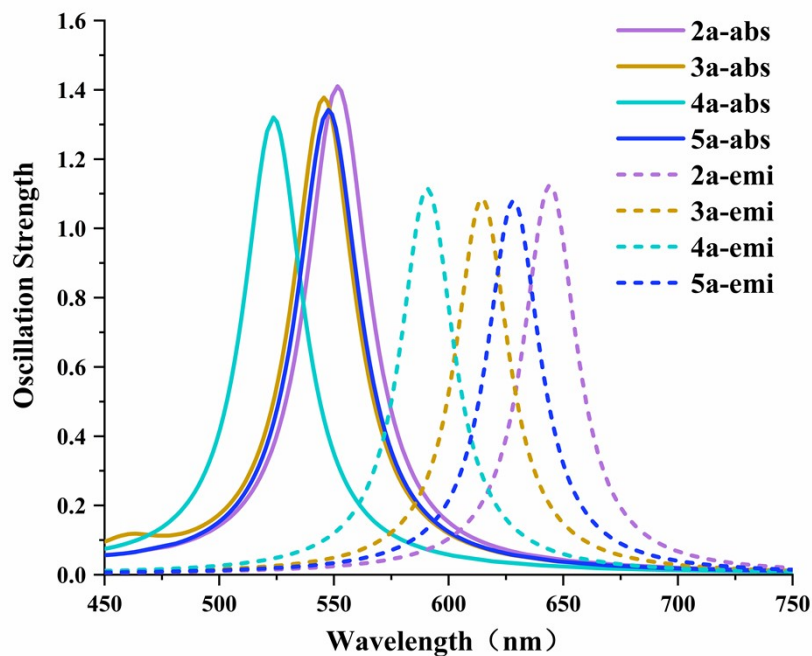


Fig. S10 The simulated one-photon absorption and fluorescence emission spectra of the studied molecules (**2a~5a**).

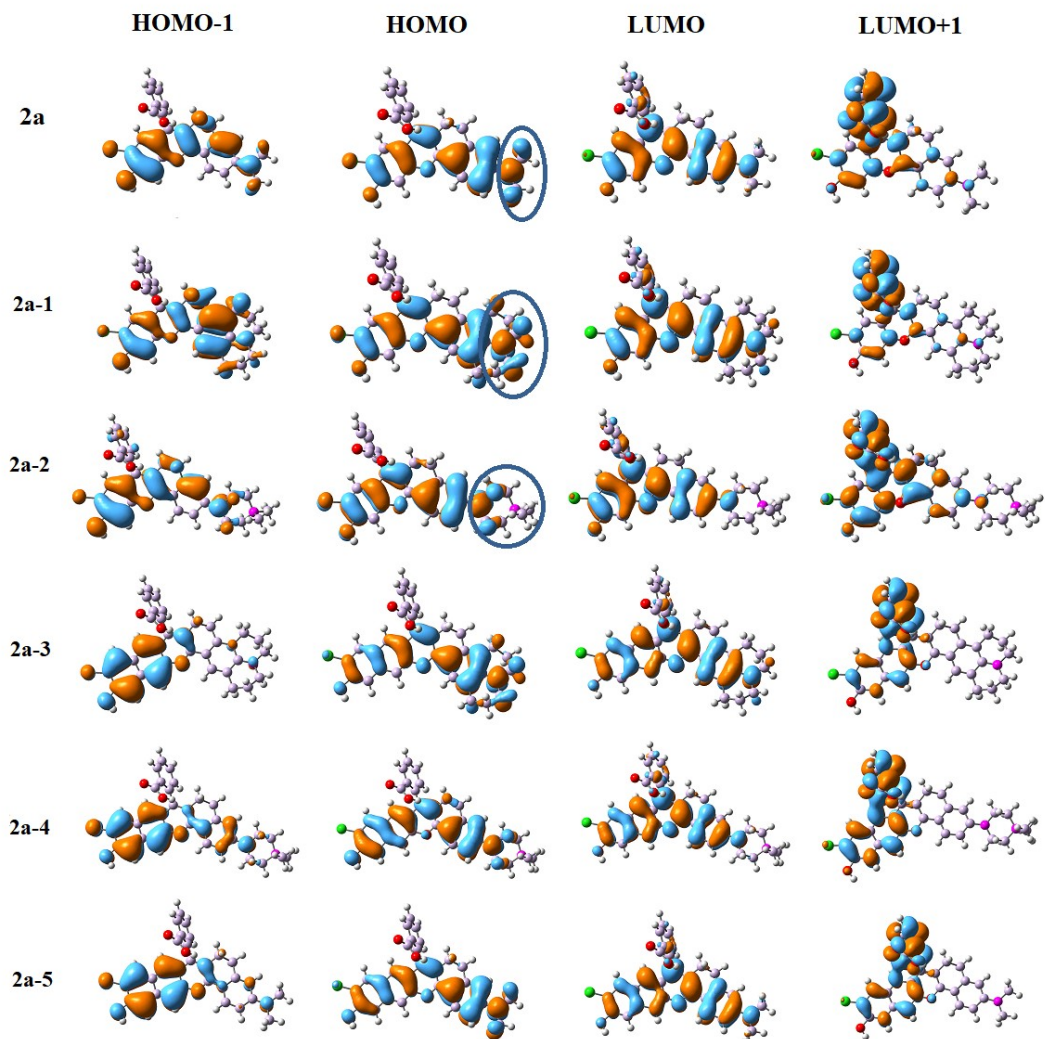


Fig. S11 The main frontier molecular orbitals of the designed molecules.

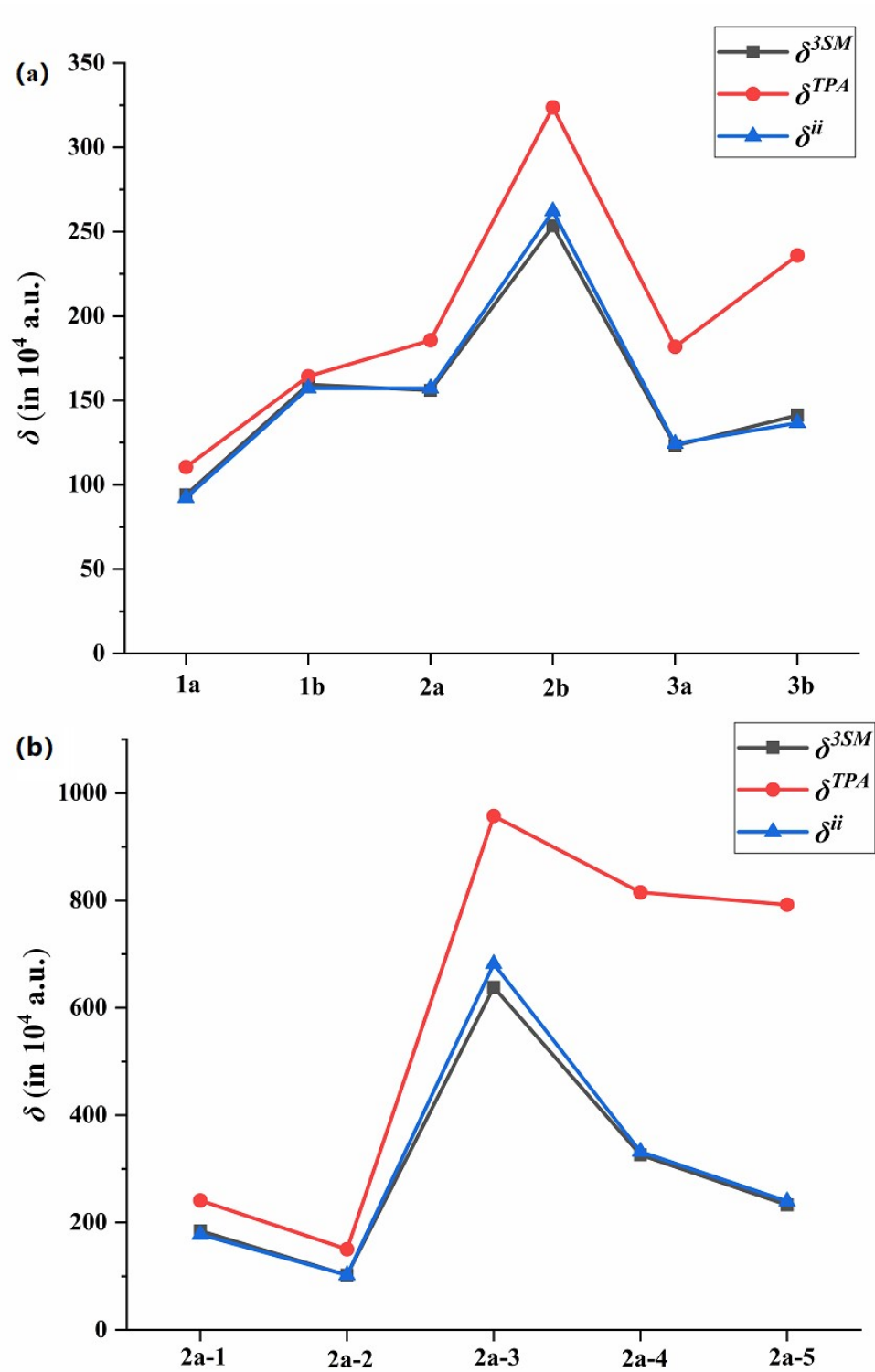


Fig. S12 Comparison between the δ^{3SM} calculated by using the three-state model and the δ^{TPA} predicted by the response theory of the studied molecules. Besides, the δ^{ii} is the first item in the three-state model formula. (a)the experimental molecules. (b)the designed molecules.

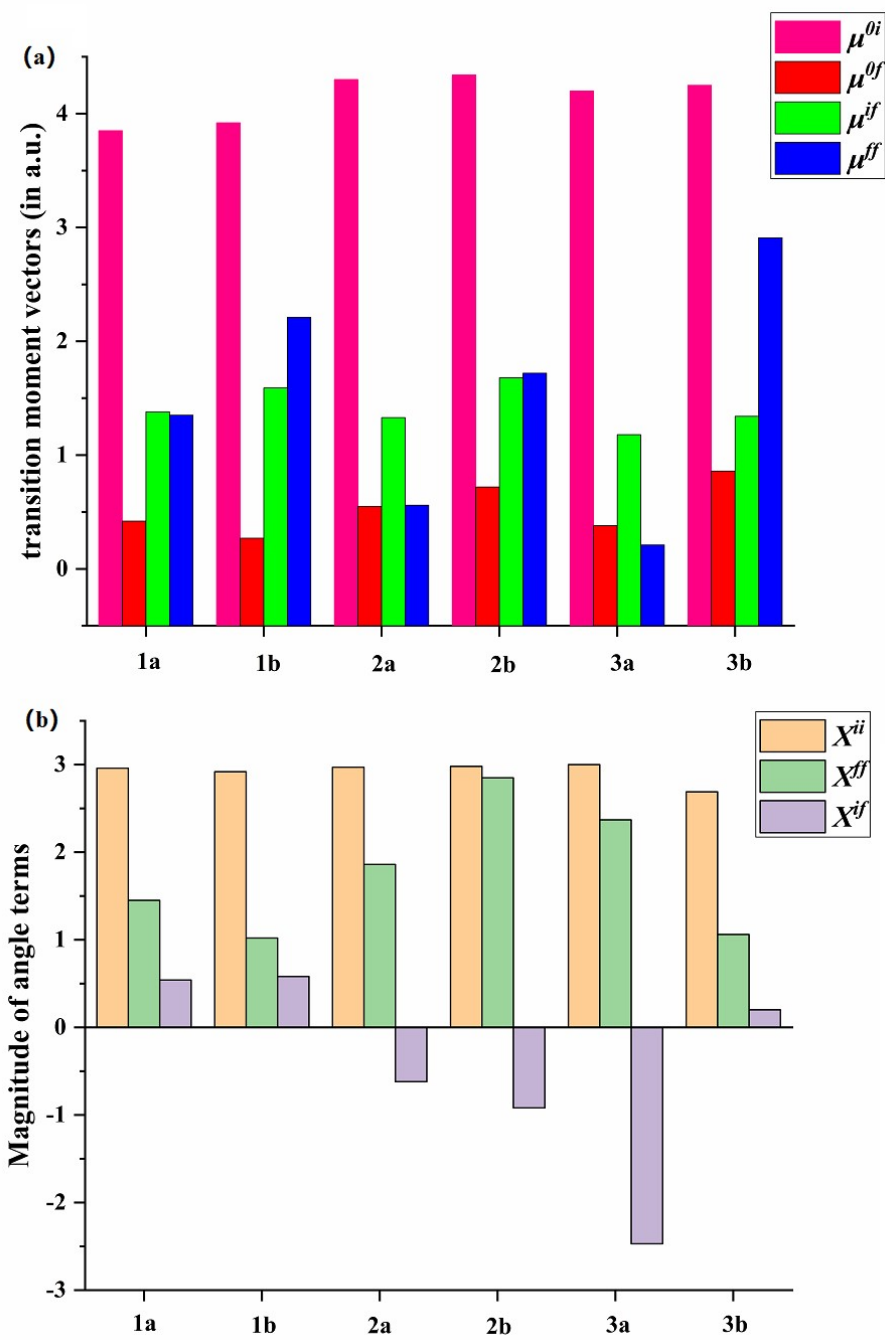


Fig. S13 Plots of (a) the dipole moment vectors μ and (b) the angle terms X existed in the 3SM of the studied experimental molecules.

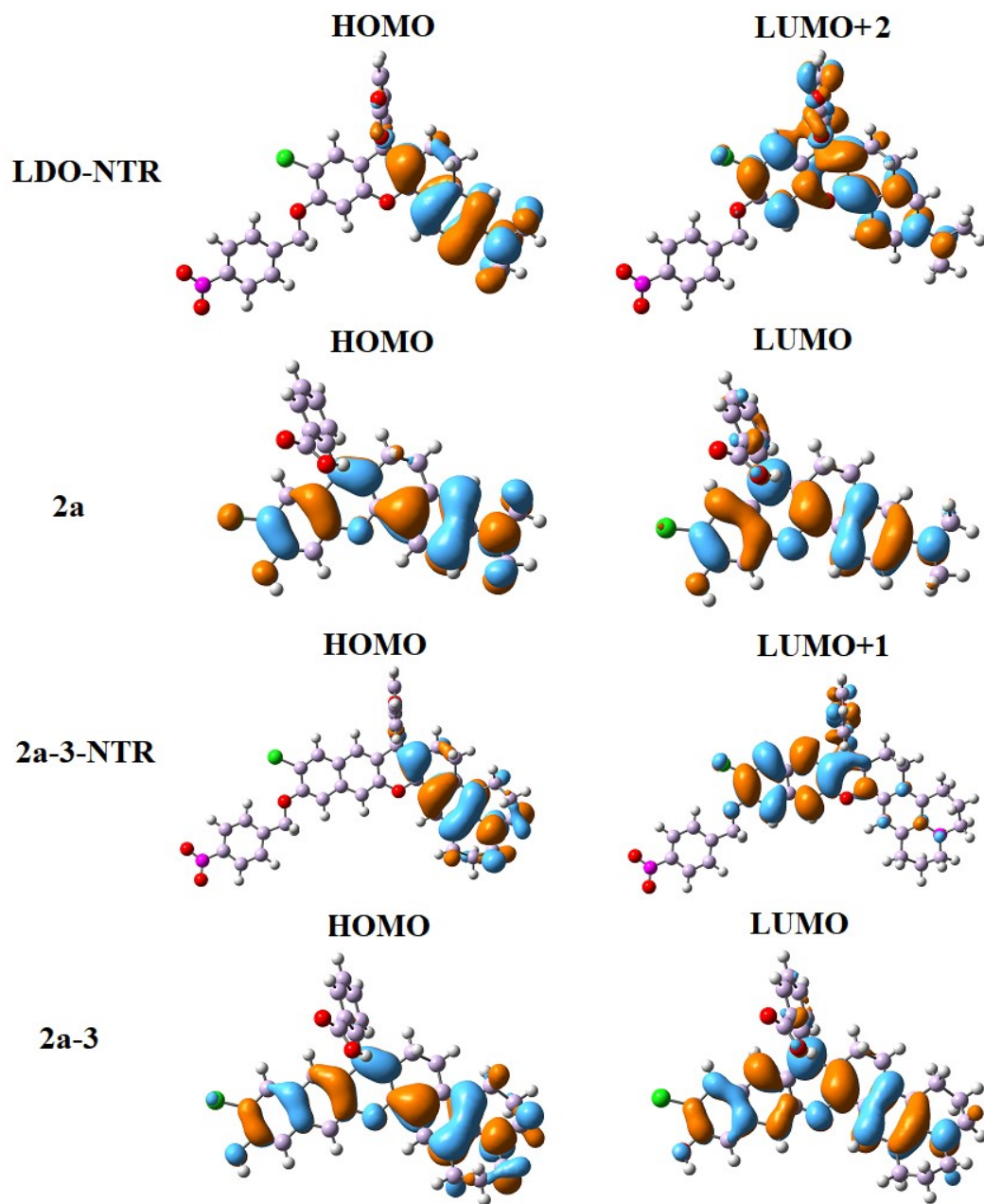


Fig. S14 The main frontier molecular orbitals of the studied probes and products.

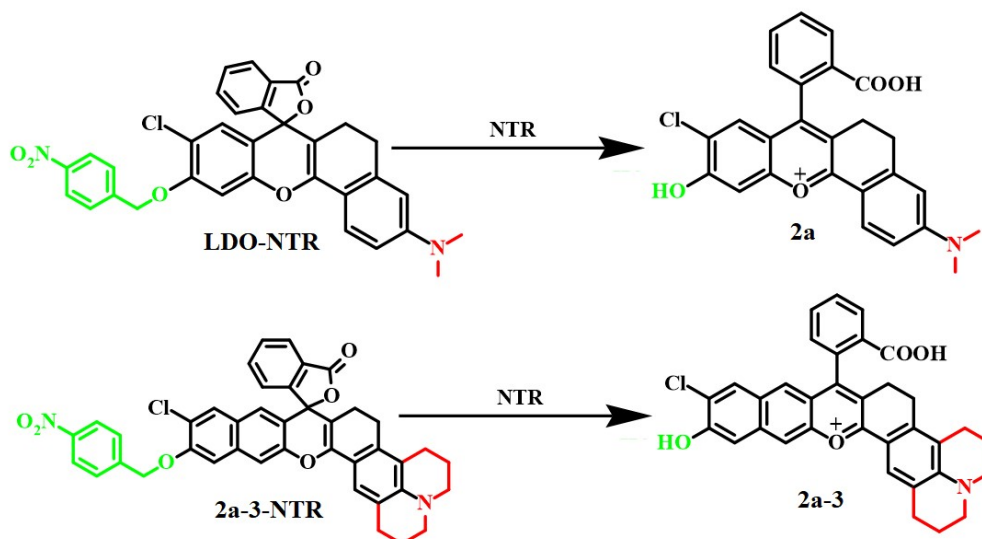


Fig. S15 Detailed division of the probes and products.(I in green, II in black, III in red)



Fig. S16 The detailed division of electron donor and electron acceptor regions for the probe **LDO-NTR** and **2a-3-NTR**, including the green is the electron acceptor and the red is the electron donor.

References

- 1 R. C. Hilborn, Einstein coefficients, cross sections, f values, dipole moments, and all that, *Am. J. Phys.*, 1982, **50**, 982–986.
- 2 M. T. P. Beerepoot, D. H. Friese, N. H. List, J. Kongsted and K. Ruud, Benchmarking two-photon absorption cross sections: performance of CC2 and CAM-B3LYP, *Phys. Chem. Chem. Phys.*, 2015, **17**, 19306–19314.
- 3 P. R. Monson and W. M. McClain, Polarization Dependence of the Two-Photon Absorption of Tumbling Molecules with Application to Liquid 1-Chloronaphthalene and Benzene, *J. Chem. Phys.*, 1970, **53**, 29–37.
- 4 W. L. Peticolas, Multiphoton Spectroscopy, *Annu. Rev. Phys. Chem.*, 1967, **18**, 233–260.
- 5 M. Albota, D. Beljonne, J.-L. Brédas, J. E. Ehrlich, J.-Y. Fu, A. A. Heikal, S. E. Hess, T. Kogej, M. D. Levin, S. R. Marder, D. McCord-Maughon, J. W. Perry, H. Röckel, M. Rumi, G. Subramaniam, W. W. Webb, X.-L. Wu and C. Xu, Design of Organic Molecules with Large Two-Photon Absorption Cross Sections, *Science*, 1998, **281**, 1653–1656.
- 6 J. Ho, A. Klamt and M. L. Coote, Comment on the Correct Use of Continuum Solvent Models, *J. Phys. Chem. A*, 2010, **114**, 13442–13444.
- 7 G. Kang, J. Ma, H. Chen, X. Ren and K. Li, Efficient structural modification of electron-withdrawing substituents on Pt(II) complexes for red emitters: A theoretical study, *Appl. Organomet. Chem.*, 2020, **34**, e5739.